

**FINITE VOLUME SCHEMES FOR TWO-PHASE  
FLOWS IN POROUS MEDIA.**

**Comparisons of some schemes for elliptic operator**

FAYSSAL BENKHALDOUN\*  
AMADOU MAHAMANE\*,

\* LAGA - Université Paris XIII

*Prague, october 31, 2007*

## PLAN

- **I- NUMERICAL SIMULATION OF WATER-OIL FLOW IN A POROUS MEDIUM**
  - Mathematical model
  - Numerical scheme
  - Numerical tests
- **II- COMPARISON OF SOME SCHEMES**
  - Presentation of the schemes
  - Comparison of the schemes from the point of view of CPU time and numerical error
- **CONCLUSION**

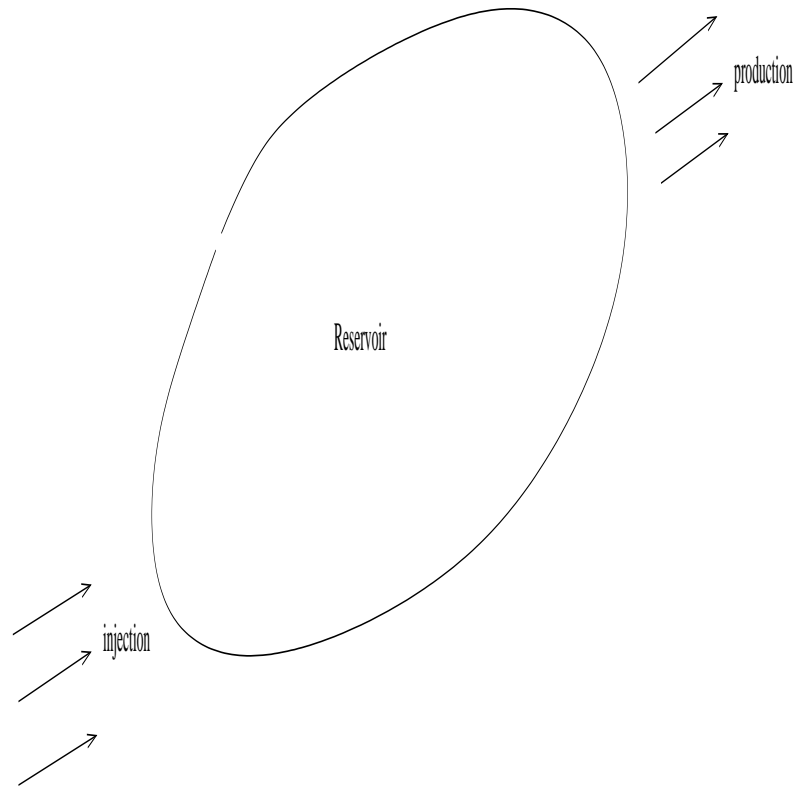
**I- NUMERICAL SIMULATION OF WATER-OIL FLOW  
IN A POROUS MEDIUM**

## MOTIVATIONS

Numerical simulation by Finite Volumes (FV) of the flow of a fluid constituted by two immiscible and incompressible phases in a porous medium. One example of such a flow is the extraction of oil by water during exploitation of oil gisements.

## MATHEMATICAL MODEL

- The tank is represented by an open set  $\Omega$  of  $\mathbb{R}^2$  with smooth by parts boundary  $\Gamma$ .  $\Gamma = \Gamma_1 \cup \Gamma_2 \cup \Gamma_3$ , where  $\Gamma_1$  is the inlet where water is injected,  $\Gamma_3$  the outlet from which oil is recovered, and  $\Gamma_2$  an impermeable part.



- **Assumptions**

1. the Darcy law applies separately for each fluid,
2. the medium is saturated by the two fluids,
3. the thermodynamic properties (density, viscosity) of the two phases are constants,
4. the capillary pressure and the permeability depend only of saturation (case where  $\Omega$  is constituted by only one type of rock),
5. the deformations of the porous medium as well as the effect of gravity are negligible.

- **The model of equations:**

Under the previous assumptions, the application of continuity law and Darcy law to each phase, leads to the system:

$$\left\{ \begin{array}{l}
 \Phi(x) \frac{\partial S_w}{\partial t} - \nabla \cdot [K(x)k_w(S_w)\nabla p_w] = 0 \text{ in } Q_T = \Omega \times [0, T[ \\
 \Phi(x) \frac{\partial S_o}{\partial t} - \nabla \cdot [K(x)k_o(S_o)\nabla p_o] = 0 \text{ in } Q_T = \Omega \times [0, T[ \\
 S = S_w, \quad S_o = 1 - S \\
 P_C = p_w - p_o = p_c(S)P_{CM} \\
 S = S_{w,M} \quad \vec{q}_w \cdot \vec{n} = -q_d \quad \text{on } \Gamma_1 \\
 \vec{q}_w \cdot \vec{n} = 0 \quad \vec{q}_o \cdot \vec{n} = 0 \text{ on } \Gamma_2 \\
 S = S_{w,m}, \quad p_o = P_{atm} \text{ and } \vec{q}_o \cdot \vec{n} > 0 \quad \text{on } \Gamma_3 \\
 S(x, 0) = S^0(x) \text{ in } \Omega
 \end{array} \right. \tag{1}$$

The above system can not be subject to a mathematical study, owing to the fact that in the area where  $S_w = S_{w,m}$ , the first equation disappears. It is one of the reasons for which **Chavent** introduced a new unknown, called **global pressure**. This leads to a system of coupled P.D.E. formed by a family of elliptic equations in pressure and by a nonlinear parabolic equation in saturation:

$$\left\{ \begin{array}{l} \vec{q} = -d(u)K(x)\nabla P; \operatorname{div}(\vec{q}) = 0 \\ \vec{q} \cdot \vec{n}|_{\Gamma_1} = -q_d; \vec{q} \cdot \vec{n}|_{\Gamma_2} = 0 \quad P|_{\Gamma_3} = P_0 \quad \forall t \in [0, T[ \end{array} \right. \quad (2)$$

$$\left\{ \begin{array}{l} \Phi(x) \frac{\partial u}{\partial t} + \operatorname{div}(b(u)\vec{q} - K(x)\nabla\alpha(u)) = 0 \text{ dans } Q_T \\ u|_{\Gamma_1} = 1; K\nabla\alpha(u) \cdot \vec{n}|_{\Gamma_2} = 0; u|_{\Gamma_3} = 0 \quad \forall t \in [0, T[ \\ u(x, 0) = u^0(x) \quad \forall x \in \Omega \end{array} \right. \quad (3)$$

whith:

$$u = \frac{S - S_{w,m}}{1 - S_{w,m} - S_{o,m}}$$

$d(u) = k_w(u) + k_o(u)$  the total mobility of the fluid,

$$\vec{q} = \vec{q}_w + \vec{q}_o$$

$$b(u) = \frac{k_w(u)}{k_w(u) + k_o(u)}$$

$$\alpha(u) = \int_0^u a(s) ds \quad \text{where } a(u) = \frac{k_w(u)k_o(u)}{k_w(u) + k_o(u)} p'_c(u) P_{CM}$$

(note that  $a(1) = a(0) = 0$ ),

$$P = \frac{1}{2}(p_w + p_o) + \delta(u) \quad \text{the global pressure}$$

$$\text{with } \delta(u) = \int_1^u (b(u) - \frac{1}{2}) p'_c(s) P_{CM} ds.$$

## THE NUMERICAL SCHEME

The temporal domain  $[0, T[$  is discretized in subintervals:  $[t_n, t_{n+1}[$  of length  $\Delta t_n$ ,  $n = 0, \dots, N_T - 1$  with  $t_0 = 0$  and  $t_{N_T} = T$ .

The space domain, Which is the tank  $\Omega$ , is discretized using a triangular non structured grid  $\mathcal{T}_h$ .

$u_C^n$  and  $P_C^n$  represent respectively a constant by cell approximation of  $u$  and  $P$  in the center of the control volume  $C$  at time  $t_n$ .

Integrating the equations (2) and (3) and applying the divergence theorem, one has **for the pressure elliptic problem:**

$$\sum_{\gamma \in \partial C} \int_{\gamma} d(u^n) K(x) \nabla P^n \cdot \vec{n}_{\gamma} ds = 0$$

for the parabolic problem:

$$\Phi_C \frac{u_C^{n+1} - u_C^n}{\Delta t_n} \text{mes}(C) = \sum_{\gamma \in \partial C} \left( - \int_{t_n}^{t_{n+1}} b(u)_\gamma \vec{q}_\gamma \vec{n}_\gamma \text{mes}(\gamma) dt \right) +$$

$$\sum_{\gamma \in \partial C \setminus \partial \Omega} \int_{t_n}^{t_{n+1}} K_\gamma \alpha'(u) \nabla u_\gamma \vec{n}_\gamma \text{mes}(\gamma) dt$$

For these two problems one needs to devise a discrete gradient on the interface of the grid cells. For this purpose a first choice is a method suggested by **Vila, Coudière et Villedieu** [1]. It consists in approximating the gradient by its average on a diamond shape Co-volume around the edge  $\gamma$ . One builds this cell diamond by connecting the barycentres of the two triangles having  $\gamma$  in common to the ends of  $\gamma$  (see figure(1)).

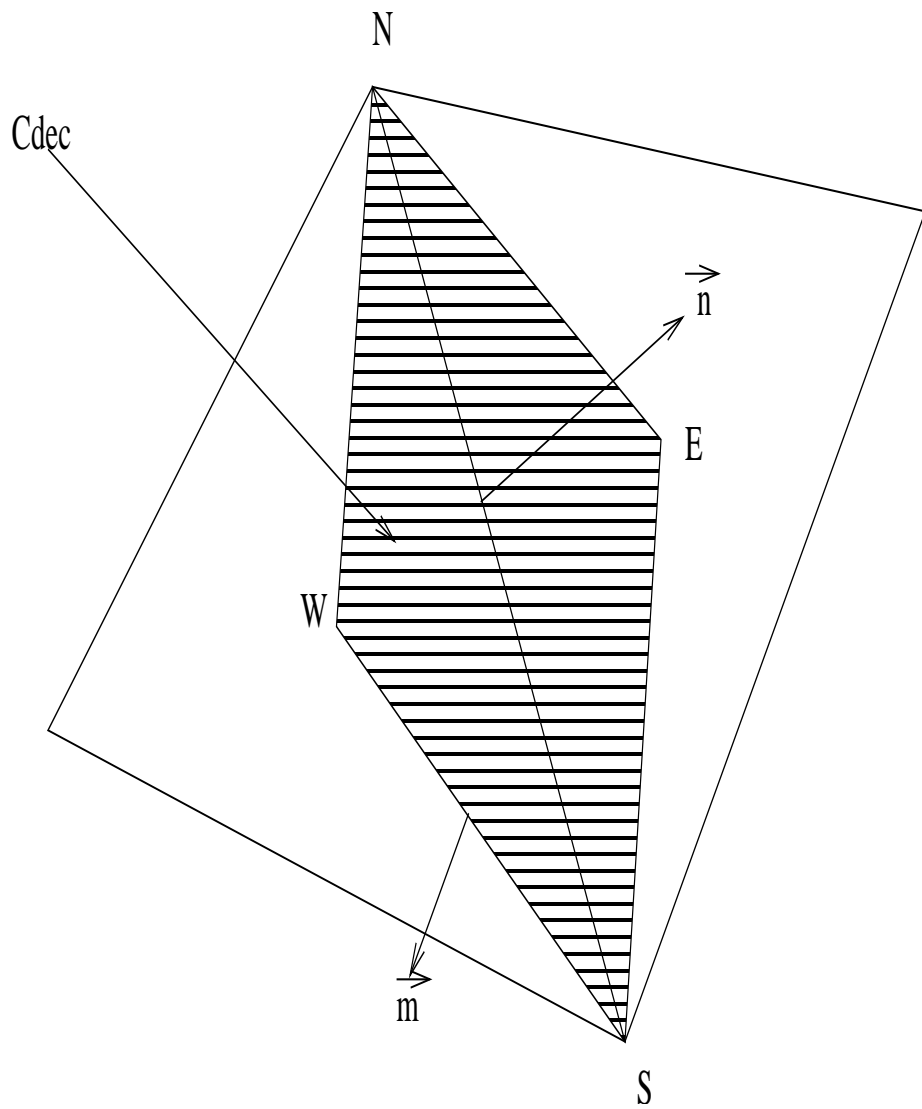


Figure 1: **Diamond co-volume**

Hence the component of the approximate gradient along x-axis writes:

$$\frac{\partial P}{\partial x} |_{\gamma} \approx \frac{1}{mes(C_{dec})} \int_{C_{dec}} \frac{\partial P}{\partial x} dx$$

(subscript  $n$  is omitted to simplify) Application of divergence theorem gives:

$$\frac{\partial P}{\partial x} |_{\gamma} \approx \frac{1}{mes(C_{dec})} \sum_{\varepsilon \in \partial C_{dec}} P|_{\varepsilon} \int_{\varepsilon} n_{x\varepsilon} d\sigma$$

$\varepsilon$  is an edge of the co-volume  $C_{dec}$  and  $n_{x\varepsilon}$  the axial component of the outer normal vector to  $\varepsilon$ .

For an edge  $\varepsilon$  of the diamond cell, let us note  $N_1$  and  $N_2$  its two ends, one then writes:  $P|_{\varepsilon} \approx \frac{1}{2}(P_{N_1} + P_{N_2})$ , where  $P_{N_1}$  and  $P_{N_2}$  are the values of the pressure  $P$  at the points  $N_1$  and  $N_2$ . Hence one has:

$$\frac{\partial P}{\partial x} |_{\gamma} \approx \frac{1}{mes(C_{dec})} \sum_{\varepsilon \in \partial C_{dec}} \frac{1}{2}(P_{N_1} + P_{N_2}) \int_{\varepsilon} n_{x\varepsilon} d\sigma$$

In an analogous way, one has:

$$\frac{\partial P}{\partial y} \Big|_{\gamma} \approx \frac{1}{mes(C_{dec})} \sum_{\varepsilon \in \partial C_{dec}} \frac{1}{2} (P_{N_1} + P_{N_2}) \int_{\varepsilon} n_{y\varepsilon} d\sigma$$

The values of  $P$  at the centers  $W$  and  $E$  are  $P_W$  and  $P_E$  while the values at the nodes  $N$  and  $S$  are interpolated or deduced from boundary conditions and are noted  $P_N$  and  $P_S$ . For a node  $N$  one has:

$$P_N = \sum_{K \in \mathcal{V}(N)} \alpha_K(N) P_K$$

where  $\mathcal{V}(N)$  is the set of triangles having in common the node  $N$ ,  $P_K$  the value of  $P$  at the center of cell  $K$  and  $\alpha_K(N)$  the interpolation weights.

These weights must verify the following conditions for the scheme to be consistent:

$$\sum_{K \in \mathcal{V}(N)} \alpha_K(N) = 1$$

$$\sum_{K \in \mathcal{V}(N)} \alpha_K(N)(x_K - x_N) = 0$$

$$\forall h > 0, \max_{K \in \mathcal{V}(N)} |\alpha_K(N)| < Cst$$

## NUMERICAL EXPERIMENTS

Two test cases have been performed. A homogeneous isotropic tank and a non homogeneous anisotropic one.

- In both cases, the initial condition  $u^0$ , the porosity  $\Phi$  and the pressure  $P_0$  are the same.

$$u^0(x) = \begin{cases} 1 & \text{if } x \in \Gamma_1 \\ 0 & \text{if } x \in \Omega \setminus \Gamma_1 \end{cases}$$

$\Phi = 0.2$  and  $P_0 = 0$ , the mobilities and the capillary pressure are given by:

$$p_c(u) = -[(1 - u)/u]^{\frac{1}{2}}$$

,

$$k_w(u) = \frac{1}{2\mu_w} u^{r_1}$$

$$k_o(u) = \frac{(1 - u)^{r_2}}{\mu_o}$$

- **homogeneous isotropic case:**

the tank  $\Omega = ]0, 0.1[ \times ]0, 0.1[$  is discretized with 3826 triangles.

A constant time step has been used:  $\Delta t = 1, 3 \cdot 10^{-6}$ ,  $q_d = 1.4$ ,

$K = Id$  where  $Id$  is the  $2 \times 2$  identity matrix

$\mu_w = 1$ ,  $\mu_o = 3$ ,  $r_1 = 5$  and  $r_2 = 3$ .

The following figures show the evolution of water saturation with time as well as velocity field distribution in the tank.

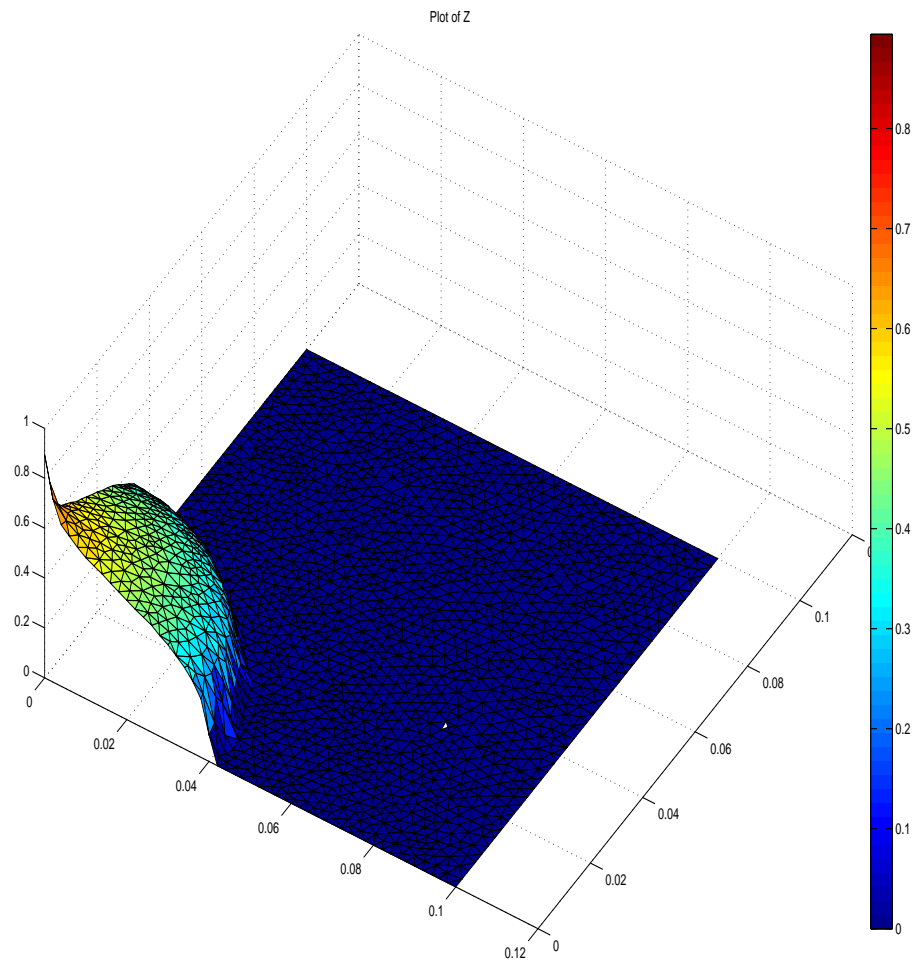


Figure 2:  $u$  at  $t = 0.016$ s

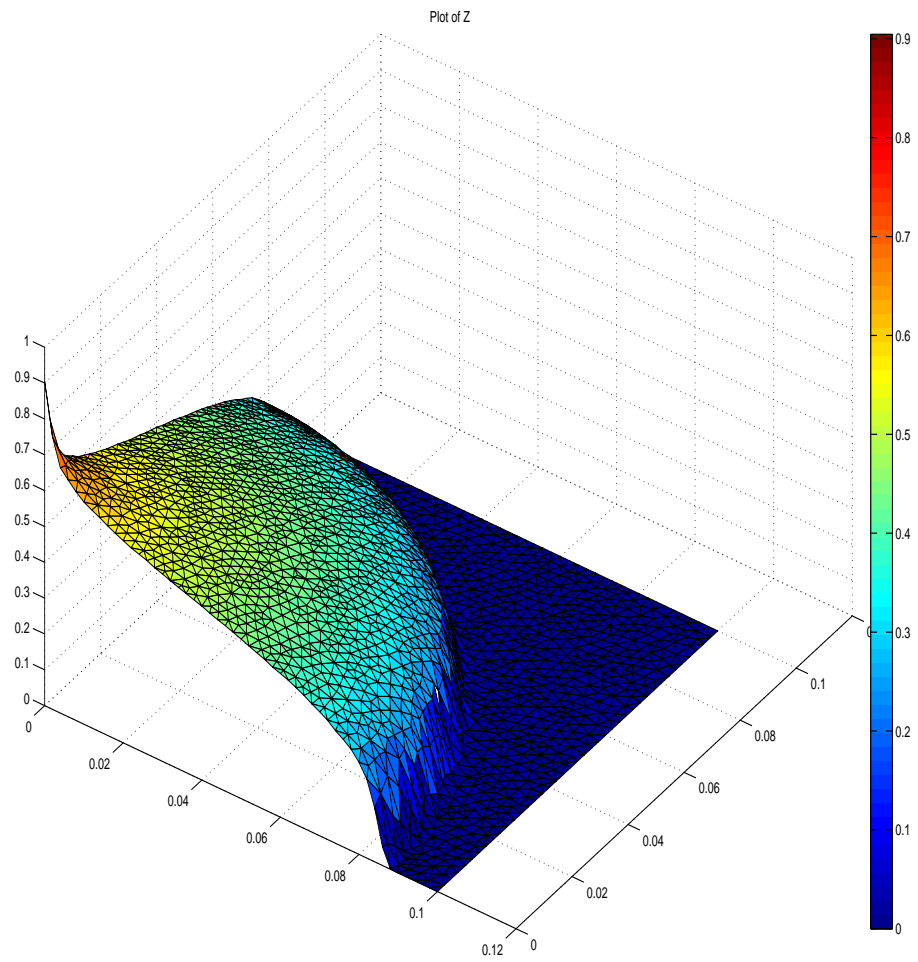


Figure 3:  $u$  at  $t = 0.08$  s

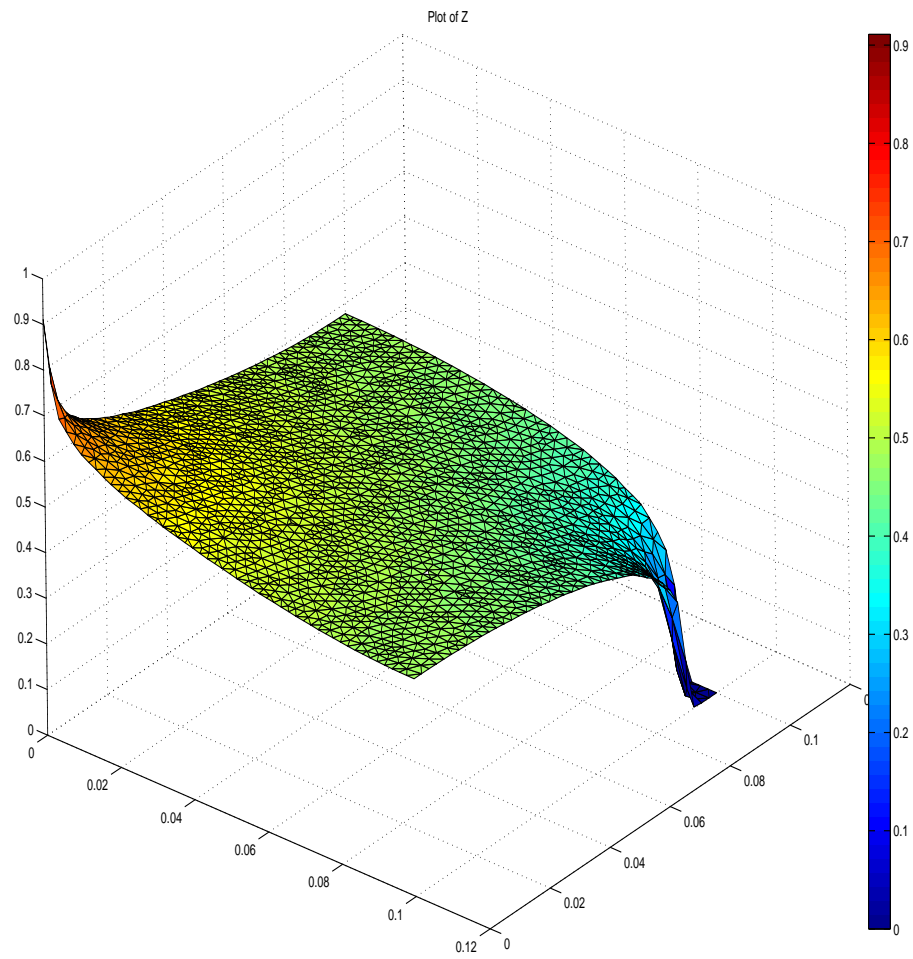


Figure 4:  $u$  at  $t = 0.176$  s

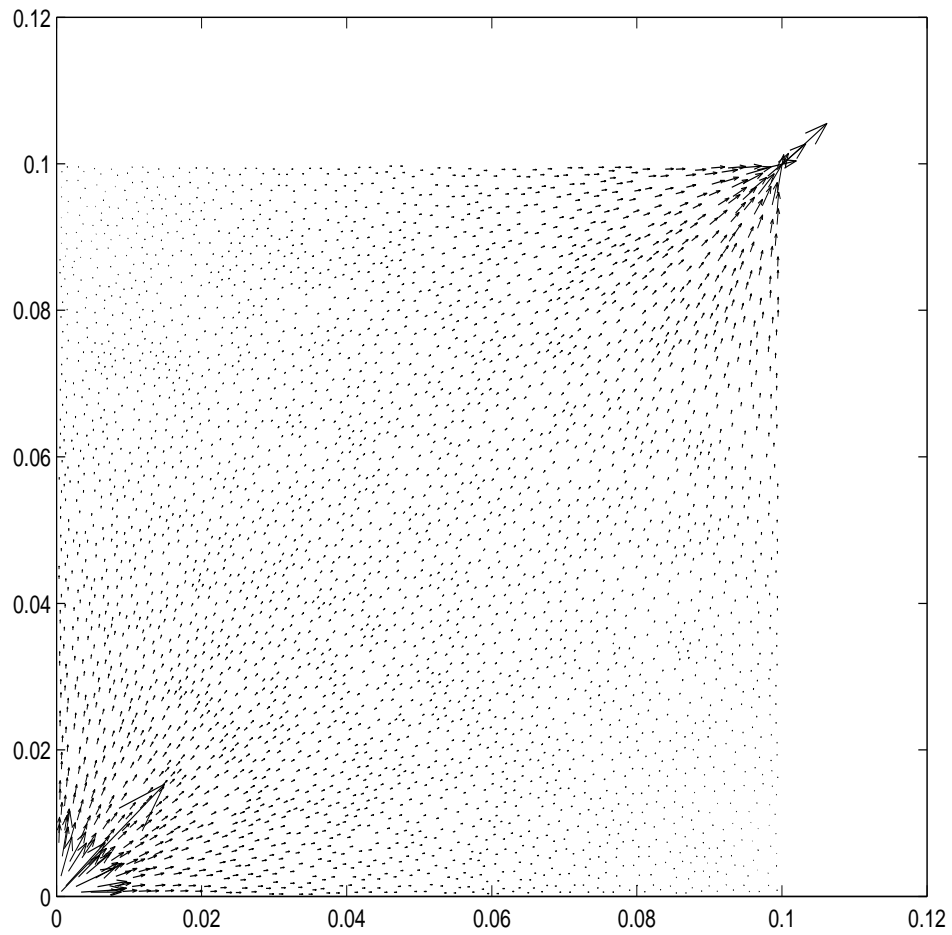


Figure 5: Velocity field in the homogeneous isotropic case

- **non homogeneous anisotropic case:**

$\Omega = ]0, 1[ \times ]0, 1[$ , is discretized using 3662 triangles, time step is  $\Delta t = 2,46.10^{-4}$ ,  $q_d = 0.5$ ,  $\mu_w = 1$ ,  $\mu_o = 10$ ,  $r_1 = 3$  et  $r_2 = 3$ , permeabilities tensor is defined as follows:

$$K(x) = \begin{cases} K_1 & \text{si } x \in Z_1 \\ K_2 & \text{sinon} \end{cases}$$

where

$$K_1 = \begin{pmatrix} 0.1 & 0.03 \\ 0.03 & 0.1 \end{pmatrix},$$

$$K_2 = \begin{pmatrix} 1 & 0.3 \\ 0.3 & 1 \end{pmatrix}$$

and  $Z_1$  is a part of  $\Omega$  defined on the figure (6).

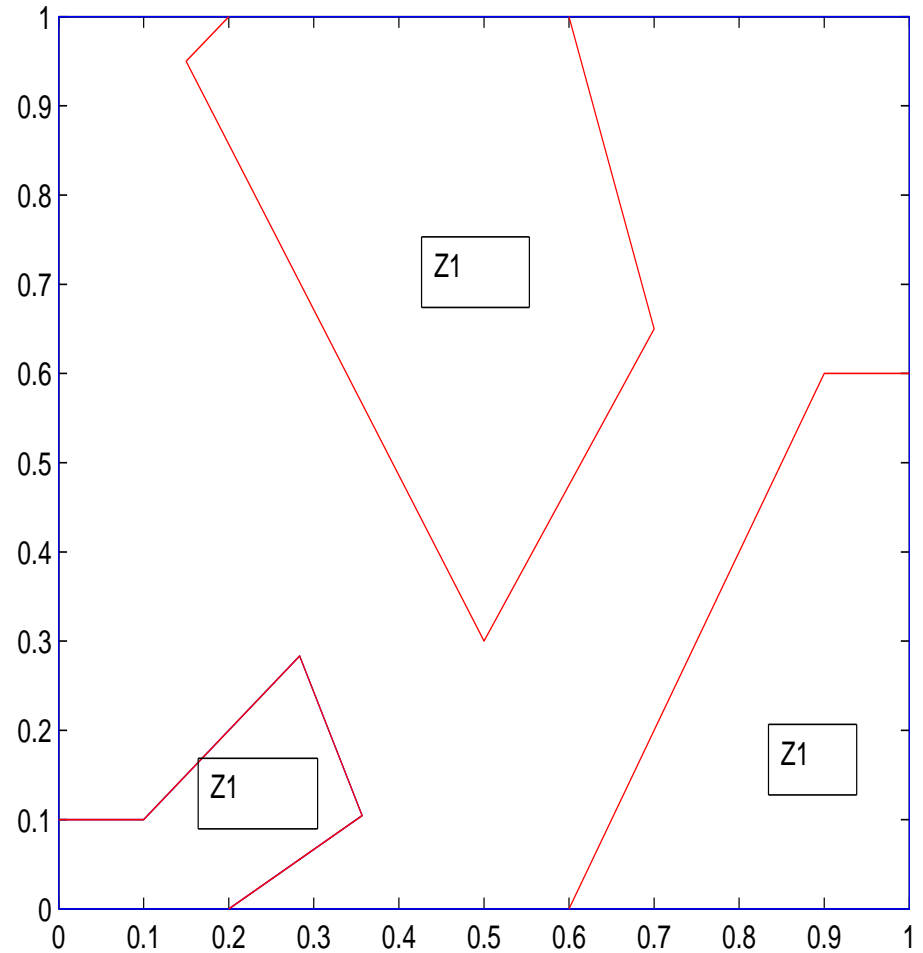
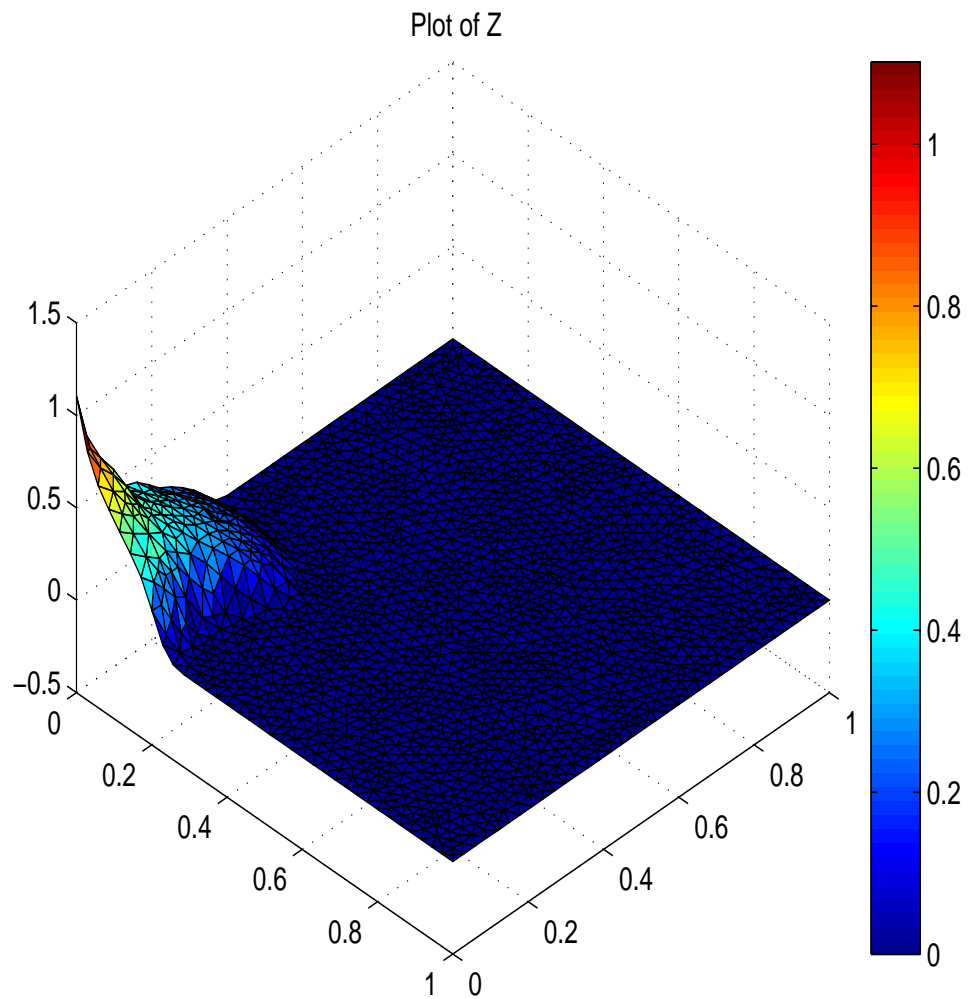
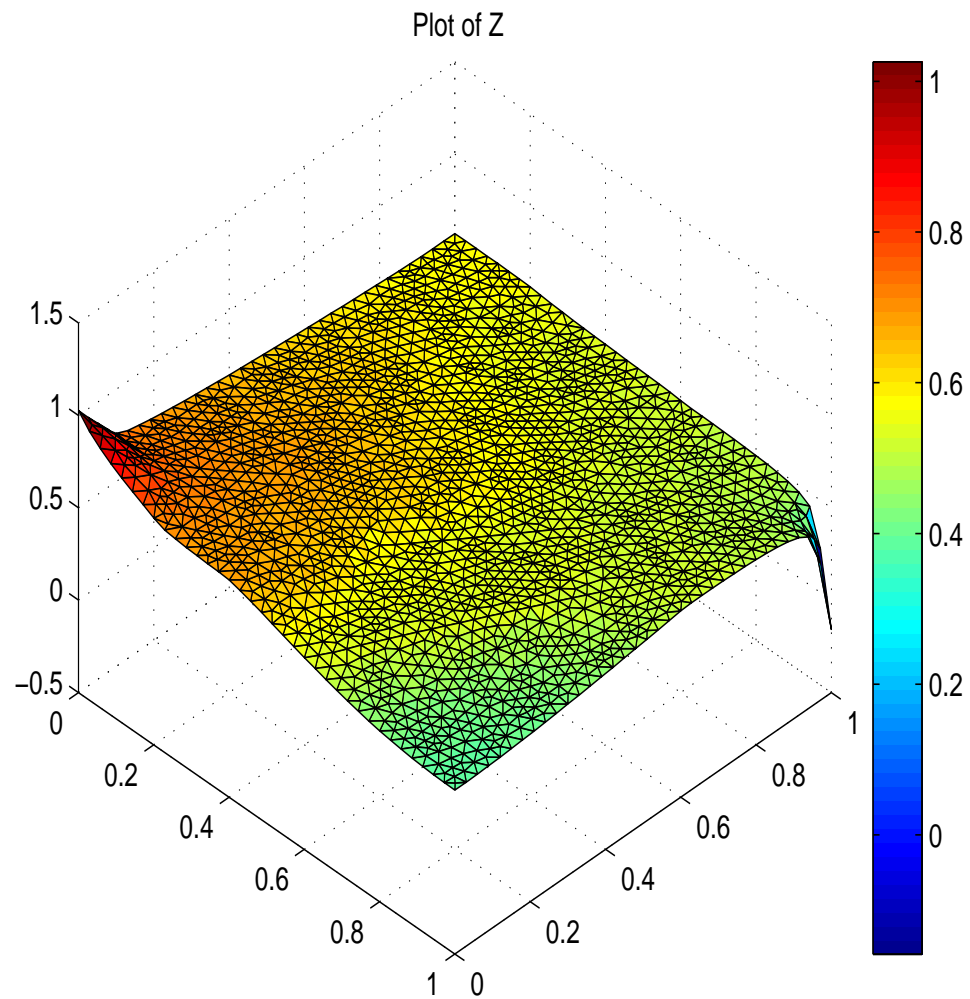


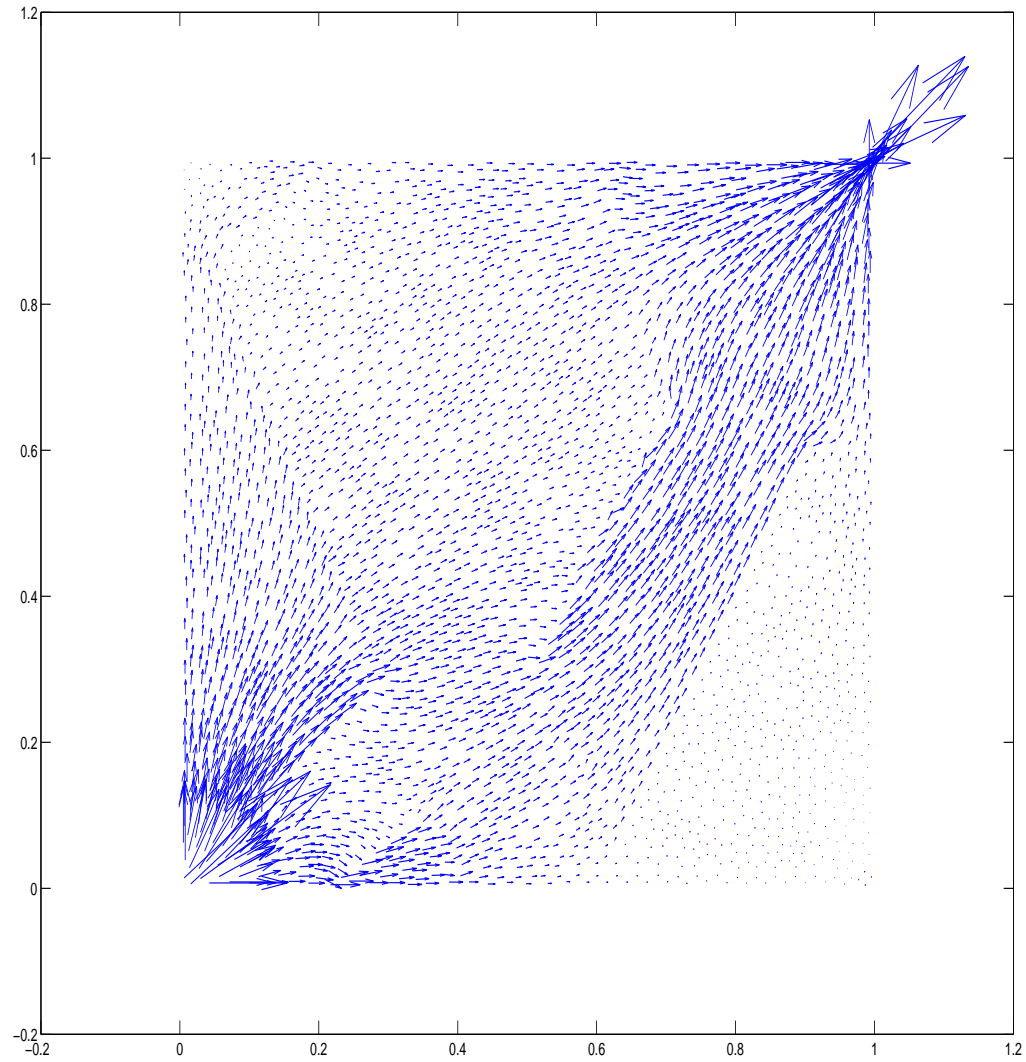
Figure 6: The tank  $\Omega$  with different permeability zones



Saturation de l'eau à  $t = 0.0492$  s



Saturation à  $t = 7.38$  s



**COMPARAISON OF DIFFERENTS SCHEMES FOR  
THE ELLIPTIC OPERATOR**

Here we make a comparison between the diamond scheme presented above and two other schemes suggested respectively by: Pascal OMNES and al. and G. MANZINI and al.

**The test case:**

$$\begin{cases} \frac{\partial u(\mathbf{x}, t)}{\partial t} - \Delta u(\mathbf{x}, t) = f(\mathbf{x}, t) & \text{in } \Omega \times ]0, T] \\ u(\mathbf{x}, t)|_{\partial\Omega} = 0 \quad \forall t \in ]0, T] \\ u(\mathbf{x}, 0) = 0 \quad \forall \mathbf{x} \in \Omega \end{cases} \quad (4)$$

If

$$f(\mathbf{x}, t) = x(1-x)y(1-y) \cos t + 2(x(1-x) + y(1-y)) \sin t$$

$$\text{with } \mathbf{x} = (x, y)$$

then:

$$u(\mathbf{x}, t) = x(1-x)y(1-y) \sin t \quad \forall (\mathbf{x}, t) \in \Omega \times ]0, T]$$

## P. OMNES SCHEME [7]

It consists of the construction of  $(\nabla_h)$ , the discrete gradient operator, and  $(\nabla_h \cdot)$  the discrete divergence operator.

### The discrete gradient:

The construction of the gradient is made in the same way as in the diamond scheme, with the difference that the values on the nodes are no more interpolated but are calculated as unknown of the problem. For this purpose one integrates on two grids, the primal triangular grid  $\mathcal{M}^T$ , and a dual grid  $\mathcal{M}^P$  obtained by joining the centers of the cells around a node of  $\mathcal{M}^T$ . This gradient is given by its values on the diamond cells:

$$(\nabla_h u)_j := \frac{1}{2\text{mes}(D_j)} \left( [u_{k_2}^P - u_{k_1}^P] \text{mes}(A'_j) n'_j + [u_{i_2}^T - u_{i_1}^T] \text{mes}(A_j) n_j \right)$$

where:

- $S_{k_1}, S_{k_2}$  are the ends of the edge  $j$  corresponding to the centers of the cells of  $\mathcal{M}^P$   $P_{k_1}, P_{k_2}$
- $T_{i_1}, T_{i_2}$  are the 2 cells of  $\mathcal{M}^T$  having in common the edge  $j$ ,  $G_{i_1}, G_{i_2}$  their gravity centers
- $D_j$  the diamond cell,
- $u_{i_\alpha}^T \approx u(G_{i_\alpha})$  and  $u_{k_\alpha}^P \approx u(S_{k_\alpha})$
- $A_j = [S_{k_1}, S_{k_2}]$  and  $A'_j = [G_{i_1}, G_{i_2}]$
- $\vec{n}_j$  the normal to  $A_j$  such that  $\overrightarrow{G_{i_1} G_{i_2}} \cdot \vec{n}_j \geq 0$
- $\vec{n}'_j$  the normal to  $A'_j$  such that  $\overrightarrow{S_{k_1} S_{k_2}} \cdot \vec{n}'_j \geq 0$

### The discrete divergence:

It is defined by its values on the two meshes  $\nabla_h \cdot := (\nabla_h^T \cdot, \nabla_h^P \cdot)$  as follows:

$$(\nabla_h^T \cdot V)_i := \frac{1}{\text{mes}(T_i)} \sum_{j \in \nu(i)} \text{mes}(A_j) V_j \cdot n_{ji}$$

$$(\nabla_h^P \cdot V)_k := \frac{1}{\text{mes}(P_K)} \left( \sum_{j \in \varepsilon(k)} \text{mes}(A'_j) V_j \cdot n'_{jk} \right)$$

$$+ \frac{1}{\text{mes}(P_K)} \left( \sum_{j \in \varepsilon(k) \cap [J - J^{\text{bord}} + 1, J]} \frac{1}{2} \text{mes}(A'_j) V_j \cdot n_j \right)$$

where:

- $J$  : is the total number of edges of the primal mesh  $\mathcal{M}^T$  and  $J^{bord}$  is the number of edges on the boundary
- $V \in (\mathbb{R}^J)^2$ , such that  $V|_{D_j} = V_j$
- $\nu(i) = \{j, \text{ such that } A_j \text{ is an edge of } T_i\}$ ,
- $\varepsilon(k) = \{j, \text{ such that } S_k \text{ is a node of } A_j\}$
- $n_{ji}$  the normal to  $A_j$  out of  $T_i$ ,
- $n'_{jk}$  the normal to  $A'_j$  out of  $P_k$

For the test case (4) an explicit version of the scheme is:

$$\begin{aligned} u_i^{n+1} &= u_i^n + \Delta t (\nabla_h \cdot (\nabla_h u^n))_i + \Delta t f_i^n \\ u_k^{n+1} &= u_k^n + \Delta t (\nabla_h \cdot (\nabla_h u^n))_k + \Delta t f_k^n \end{aligned}$$

## G. MANZINI SCHEME [6]

It is an alternative of the diamond scheme. It is distinguished from this one by the conditions imposed on the weights for the interpolation on the nodes, and a nonlinear approximation of the gradient on the diamond cell.

### Conditions on the weights

- $C_{grid} \leq \alpha_K(P) < 1 \forall K \in \mathcal{V}(P)$
- $\sum_{K \in \mathcal{V}(P)} \alpha_K(P) = 1$
- $\sum_{K \in \mathcal{V}(P)} \alpha_K(P)(x_K - x_P) = 0$

### Approximation of the gradient

The gradient  $G_{ij}(u_h)$  on the interface  $f_{ij} = T_i \cap T_j$  is approximated as follows:

$$G_{ij}(u_h) = w_{ij}(u_h)\tilde{G}_{ij}(u_h) + w_{ji}(u_h)\tilde{G}_{ji}(u_h)$$

where:

$$\tilde{G}_{ij}(u_h) = \frac{u_{ij} - u_i}{h_{ij}} n_{ij} + \{\text{the tangential term}\},$$

$$u_i \approx u(x_i),$$

$$u_{ij} \approx u(x_{ij}),$$

$$n_{ij} = \text{the normal to } f_{ij} \text{ out of } T_i,$$

$$h_{ij} = (x_{ij} - x_i) \cdot n_{ij},$$

$$x_i = \text{the gravity center of the cell } T_i,$$

$$x_{ij} = \text{orthogonal projection of } x_i \text{ on } f_{ij}.$$

The explicit version of this scheme for the problem (4) writes:

$$u_i^{n+1} = u_i^n + \frac{\Delta t}{\text{mes}(T_i)} \sum_{j \in \nu(i)} G_{ij}(u_h^n) \cdot n_{ij} \text{mes}(f_{ij}) + \Delta t f_i^n$$

## COMPARISON BETWEEN EXACT SOLUTION AND THE SOLUTION GIVEN BY THE DIFFERENT SCHEMES

For  $T = 1.5$  and on the same grid we implement the 3 schemes. Figure 7 represents a cut in  $Y = 0.5$  of each of the calculated solutions and that of the exact solution. The solution calculated by the schem of OMNES is the closest one to exact solution.

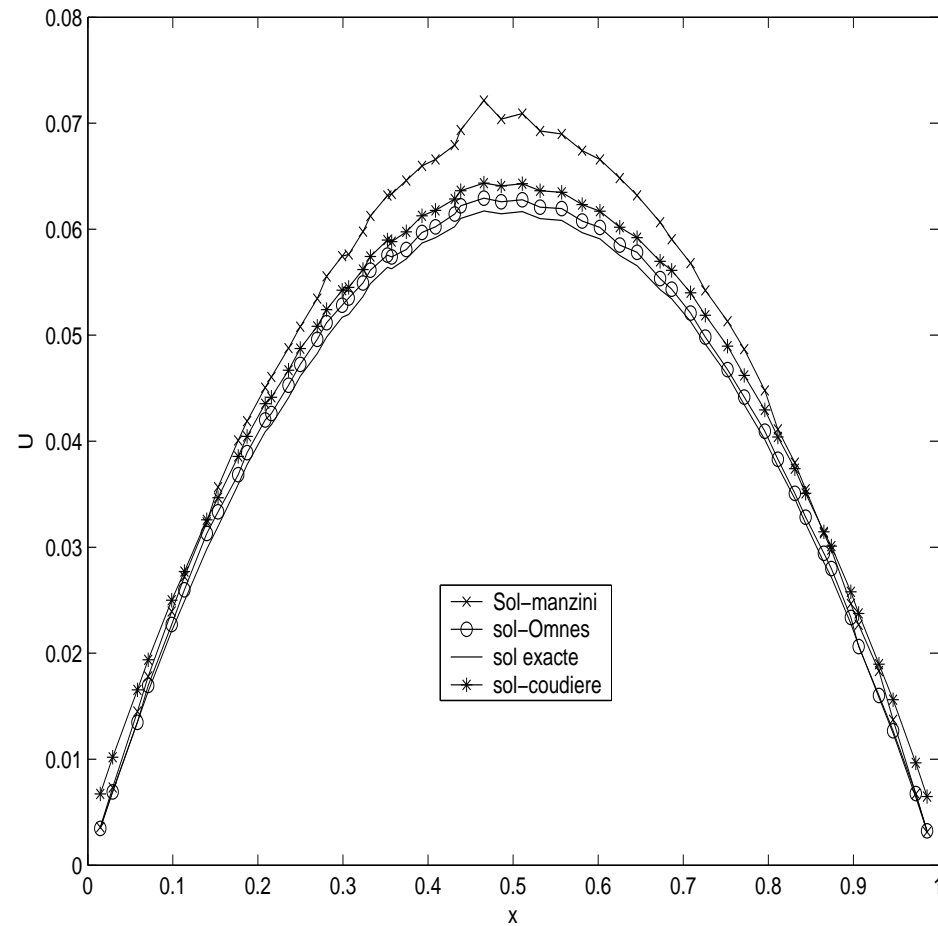


Figure 7: Comparison between exact solution and numerical solutions at  $T = 1.5$

## COMPARISON OF CPU TIME

In the table bellow CPU times are marked for each scheme on the same mesh and for the same final time  $T = 1$ ,

Schemes	Coudière	Manzini	Omnès
Temps CPU	<b>3.024s</b>	5.264 s	4.588 s

## BEHAVIOUR OF $L^1$ ERREOR IN TIME

For a fixed grid we mark the  $L^1$  error for different times of simulation: 0.3, 0.6, 0.9, 1.2, 1.5, and we observe the evolution of the error for each scheme:

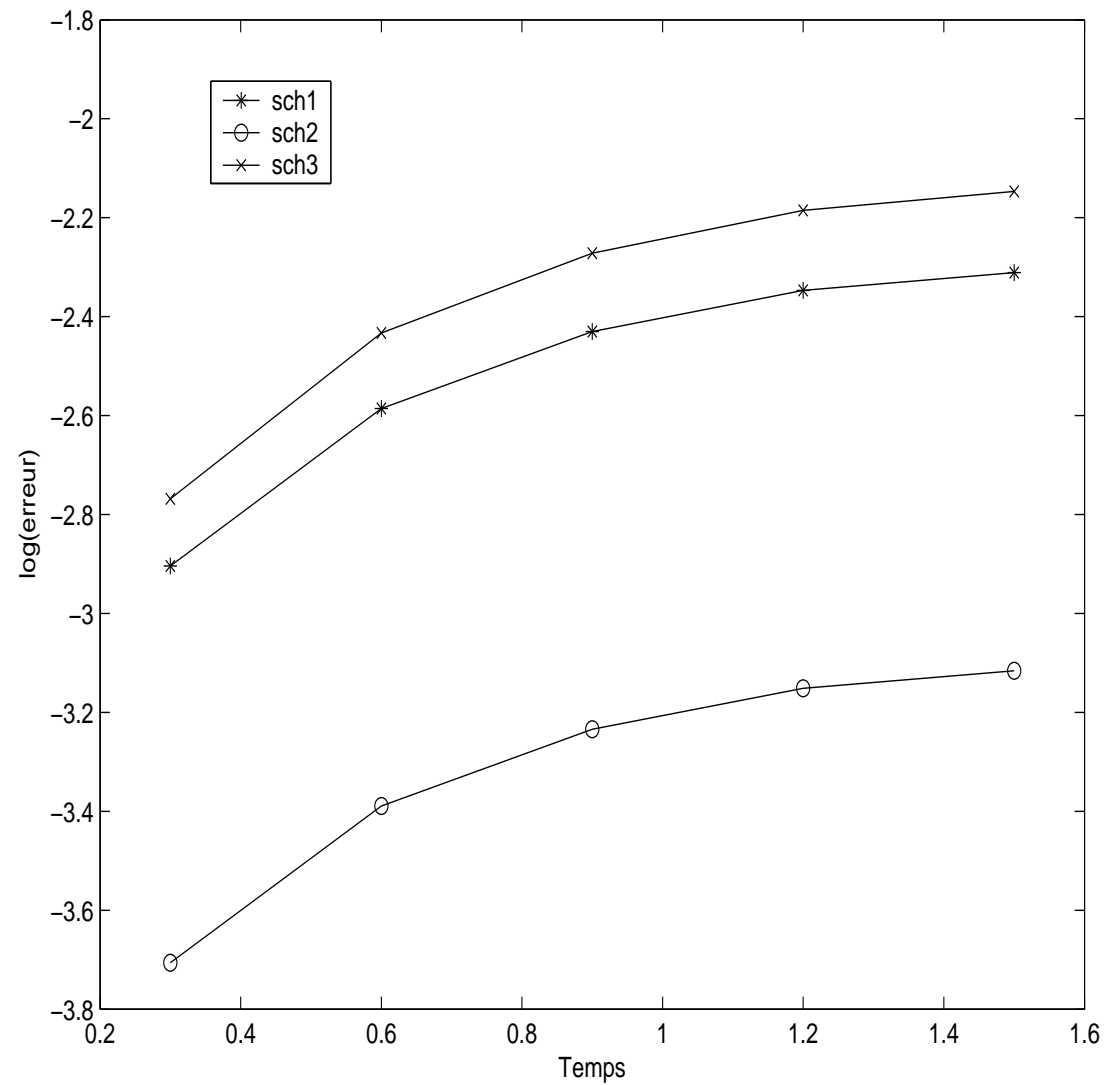


Figure 8:  $L^1$  error as a function of time

## ORDER OF CONVERGENCE

We fix the final time  $T$  to 0.1, the spatial domain  $\Omega$  is refined 5 times.

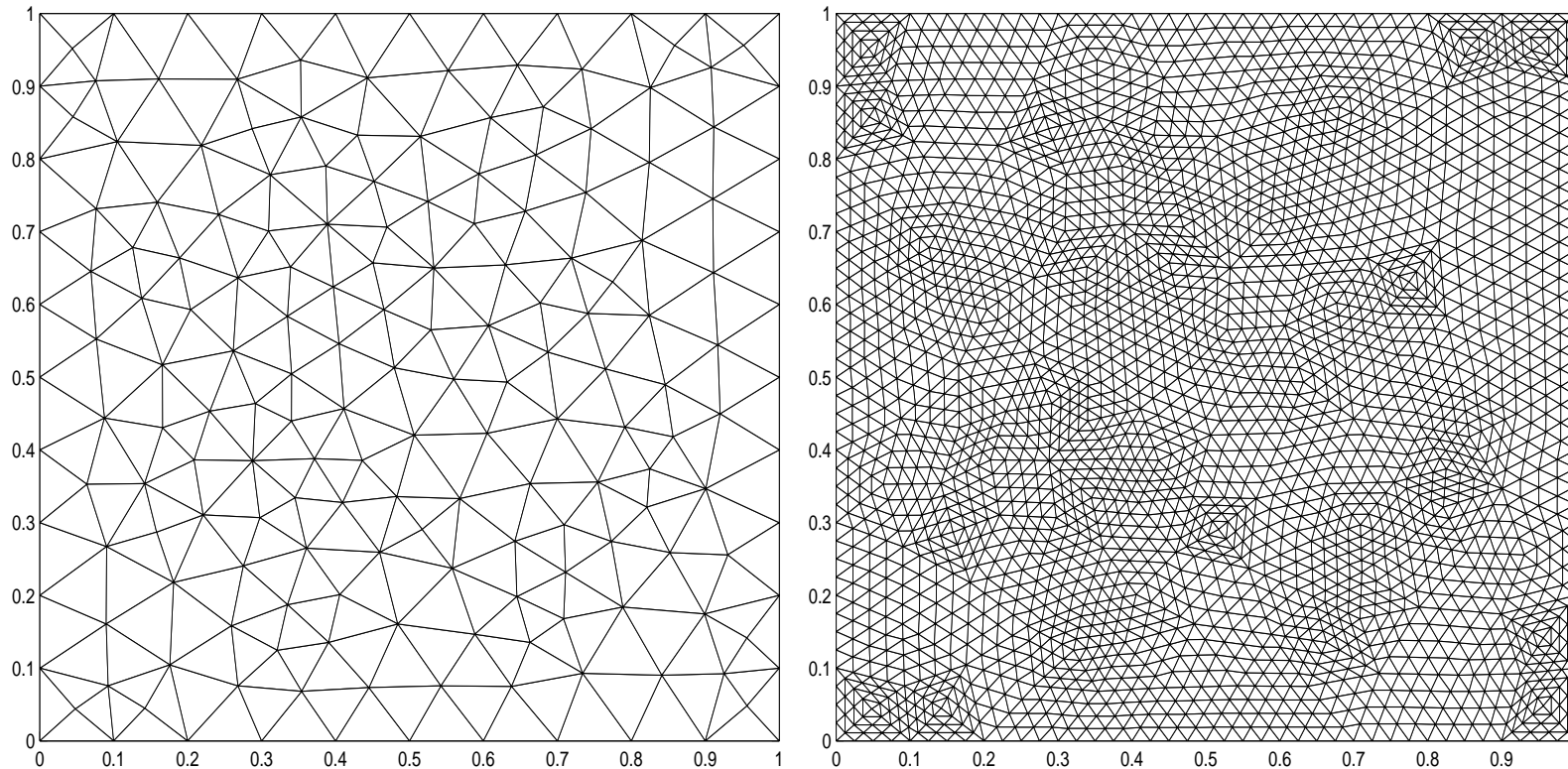


Figure 9: the initial mesh (coarse) and the mesh refined two times

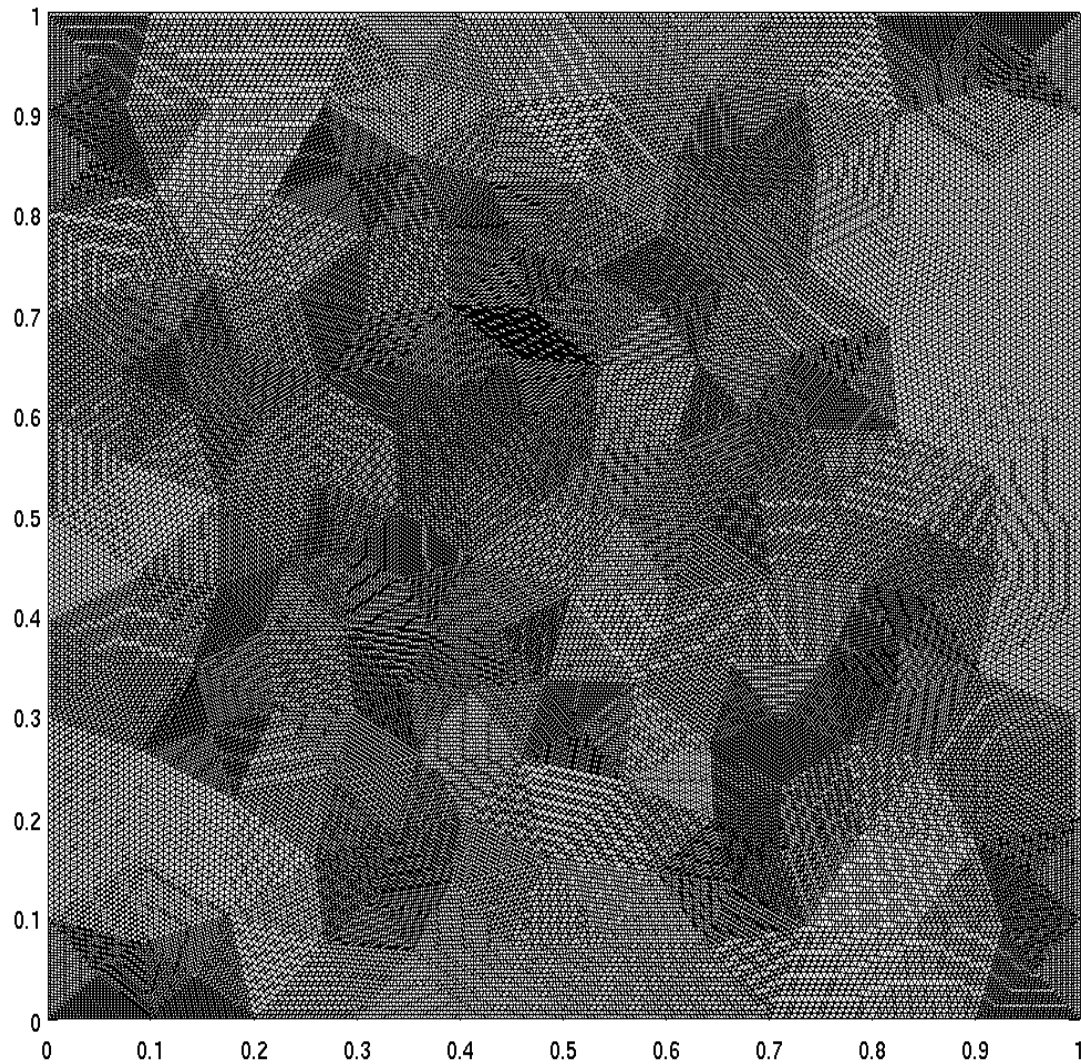


Figure 10: finest mesh

The following figures represent the log of the  $L^2$  error as a function of the log of the step  $h = \max_K \delta(K)$  where  $\delta(K)$  indicates the diameter of  $K$ . They show that the diamond scheme has the highest order of convergence.

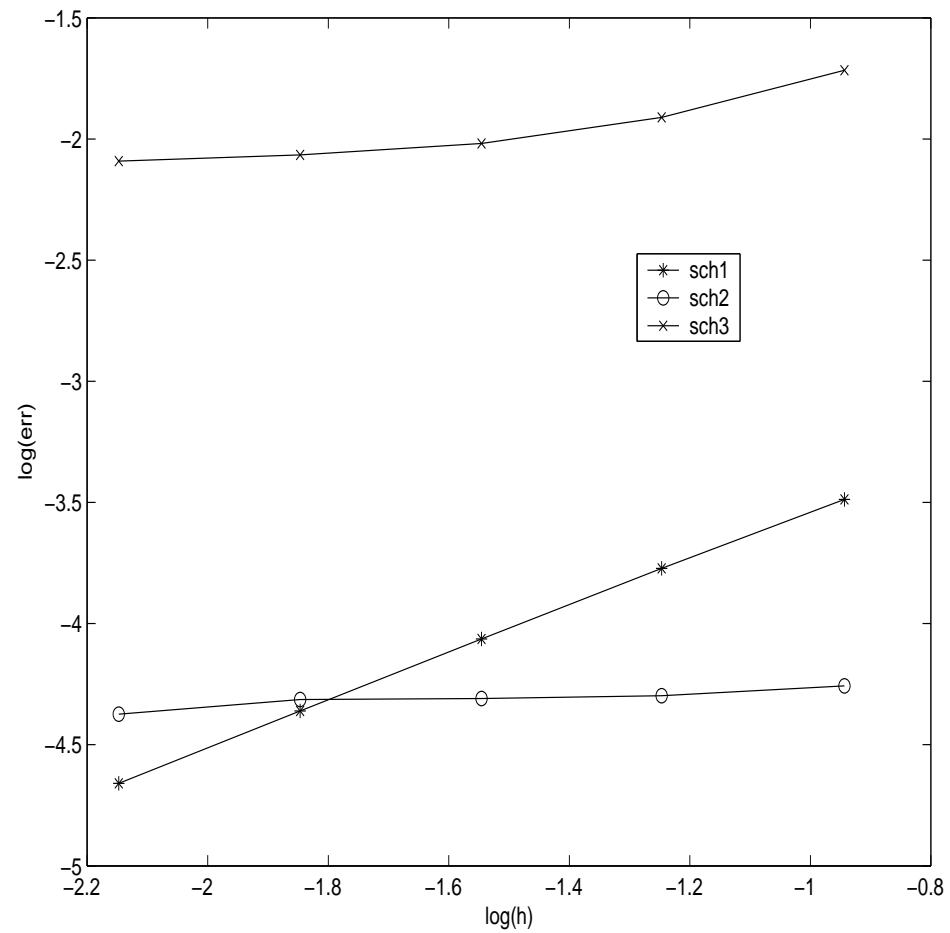


Figure 11:  $L^2$  error as a function of  $h$  for the 3 schemes

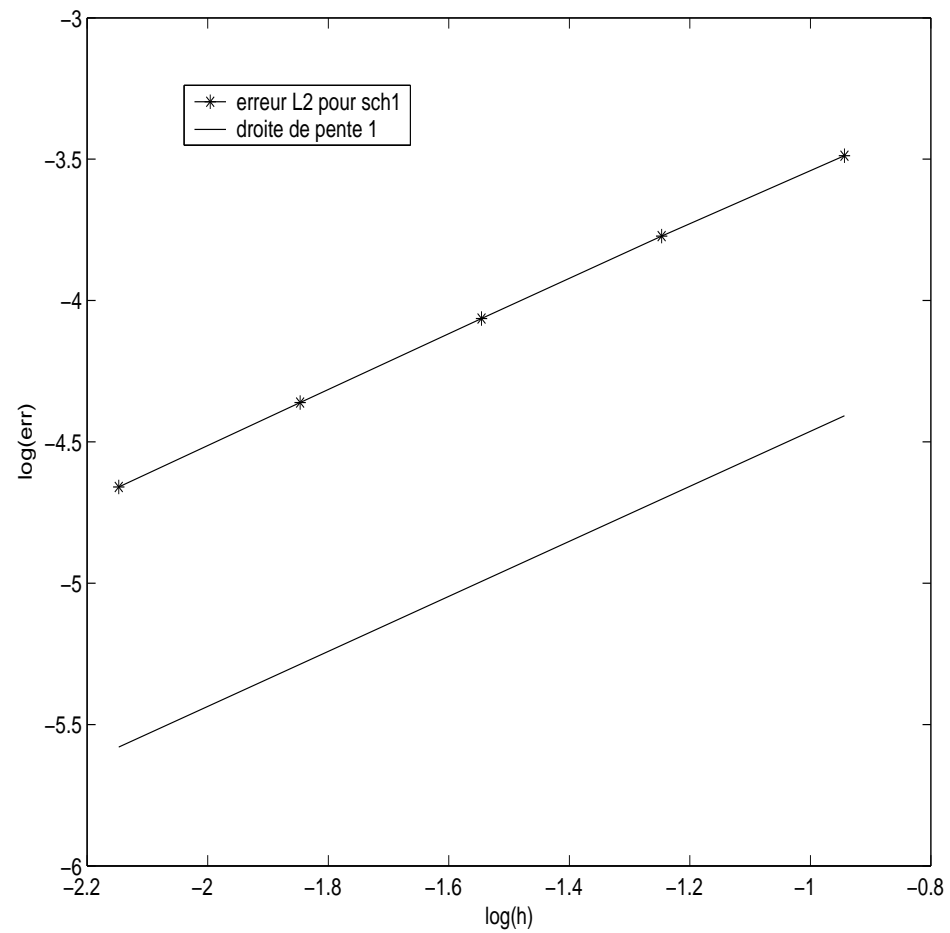


Figure 12:  $L^2$  error plot as a function of  $h$  for **Diamond** scheme

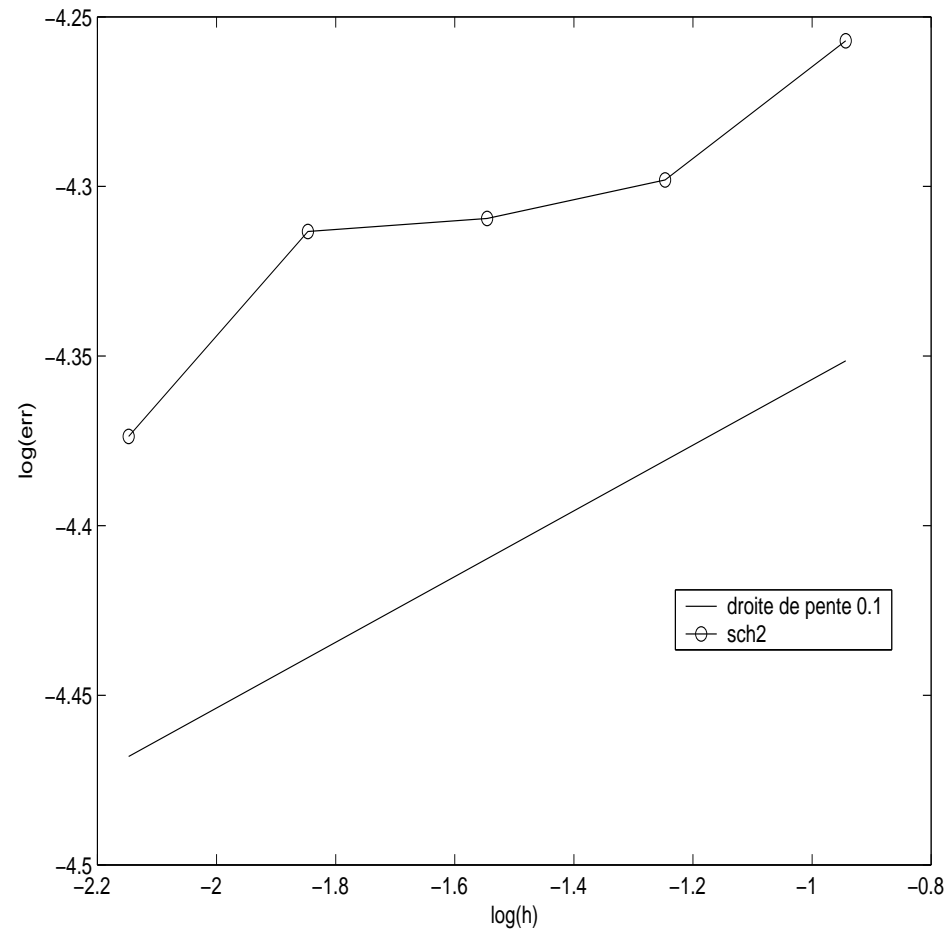


Figure 13:  $L^2$  error plot as a function of  $h$  for **Omnes scheme**

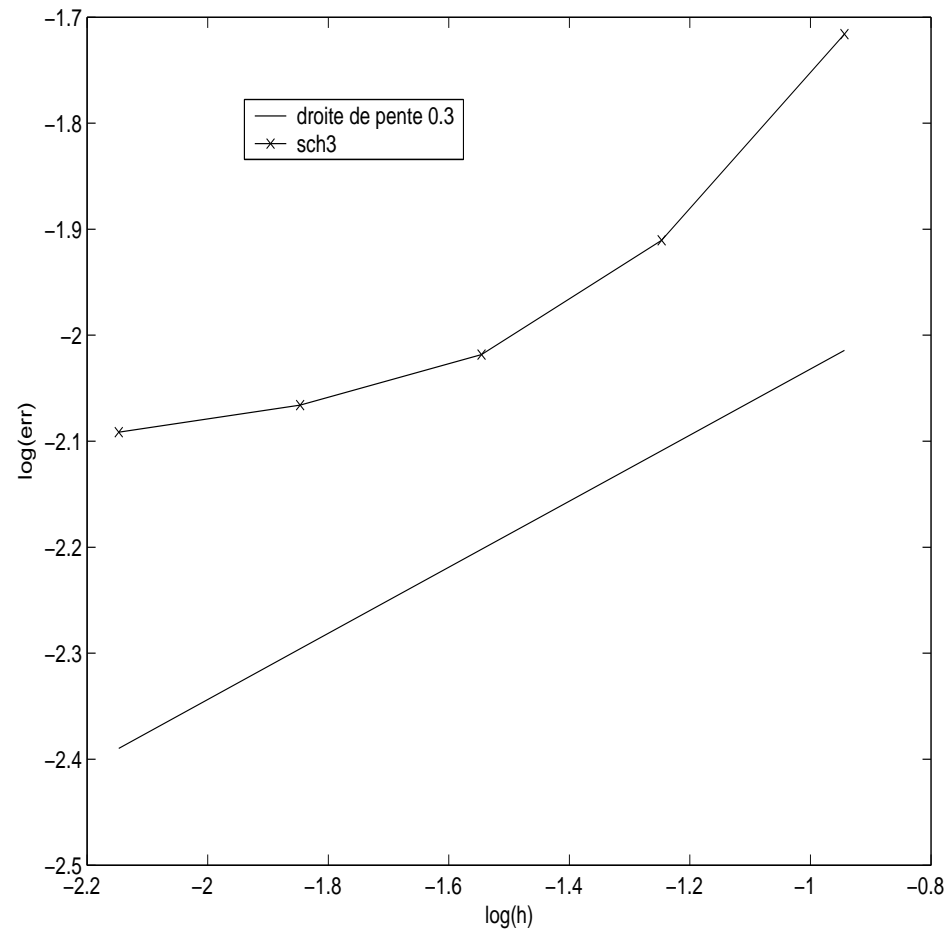


Figure 14:  $L^2$  error plot as a function of  $h$  for **Manzini** scheme

## CONCLUSION

- Treatment of the elliptic and parabolic equation by a Finite Volume scheme
- Robust scheme able to deal with heterogeneities and anisotropy
- The compared numerical study shows that the scheme of Coudiere seems to be a good compromise of the different schemes

## References

- [1] Y. COUDIÈRE, J. P. VILA AND P. VILLEDIEU, *Convergence rate of finite volume scheme for a two dimensional convection-diffusion problem*, M2AN, Vol.33 N3, p.493-516,1999.
- [2] G. CHAVENT, J. JAFFRÉ, *Mathematical Models and Finite Element for Reservoir Simulation*, North-Holland, 1986.
- [3] MOHAMED AFIF, *Schémas Volumes Finis pour une Classe d'Equations de Type Convection-Diffusion Issue des Milieux Poreux*, Thèse d'Etat UNIVERSITE CADI AYYAD MARRAKECH, 2002.
- [4] M. AFIF, *Convergence of finite volume schemes for degenerate convection-diffusion equation arising in flow in porous media*, Comput. Methods Appl. Mech. Engrg,192, 2002.

- [5] GERARD L.G. SLEIJPEN AND DIEDERIK R. FOKKEMA, *Bicgstab(1) for linear equations involving unsymmetric matrices with complex spectrum*, Electronic Transaction on Numerical Analysis, Vol. 1, pp 11-32, September 1993.
- [6] ENRICO BERTOLAZZI AND GIANMARCO MANZINI, *A second-order maximum principle preserving finite volume method for steady convection-diffusion problems*, SIAM J. NUMER. ANAL., Vol. 43 No. 5 pp. 2172-2199, 2005.
- [7] KOMLA DOMELEVO AND PASCAL OMNES, *A finite volume method for the laplace equation on almost arbitrary two-dimensional grids*, M2AN, vol. 39, No. 6, 2005, pp. 1203-1249.
- [8] R. EYMARD, T. GALLOUËT AND R. HERBIN, *Hand book of*

*Numerical Analysis* Vol. 7, P.G. Ciarlet and J.-L. Lions, Eds., North-Holland/Elsevier, Amsterdam (2000) 713-1020.

- [9] R. EYMARD, *Two-phase flow in porous media and finite volume schemes*, in F. Benkhaldoun and R. Herbin eds *Finite Volumes for Complex Application III* 2001.

**MERCI POUR VOTRE ATTENTION**